

Transmissive Nanohole Arrays for Massively-Parallel Optical Biosensing

Yanan Wang,[†] Archana Kar,[‡] Andrew Paterson,[‡] Katerina Kourentzi,[‡] Han Le,[†] Paul Ruchhoeft,[†] Richard Willson,^{*,‡,§} and Jiming Bao^{*,†}

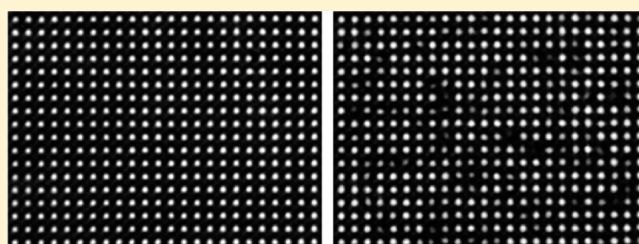
[†]Department of Electrical and Computer Engineering and [‡]Department of Chemical and Biomolecular Engineering, University of Houston, Houston, Texas 77204, United States

[§]Centro de Biotecnología FEMSA, Departamento de Biotecnología e Ingeniería de Alimentos, Tecnológico de Monterrey, Monterrey, NL 64849, Mexico

S Supporting Information

ABSTRACT: A high-throughput optical biosensing technique is proposed and demonstrated. This hybrid technique combines optical transmission of nanoholes with colorimetric silver staining. The size and spacing of the nanoholes are chosen so that individual nanoholes can be independently resolved in massive parallel using an ordinary transmission optical microscope, and, in place of determining a spectral shift, the brightness of each nanohole is recorded to greatly simplify the readout. Each nanohole then acts as an independent sensor, and the blocking of nanohole optical transmission by enzymatic silver staining defines the specific detection of a biological agent. Nearly 10000 nanoholes can be simultaneously monitored under the field of view of a typical microscope. As an initial proof of concept, biotinylated lysozyme (biotin-HEL) was used as a model analyte, giving a detection limit as low as 0.1 ng/mL.

KEYWORDS: nanohole array, transmission optical microscope, immunoassay, biosensing, enzymatic silver staining, colorimetric detection



Nanoholes in noble metal films have been frequently used in optical detection of chemical and biological agents since the discovery of the phenomenon of extraordinary optical transmission (EOT), whereby subwavelength nanoholes in plasmonic films transmit light far more efficiently than would classically be expected.^{1–5} Depending on the type of light source and the optical detection method, two configurations typically are employed. One approach measures the peak shift of the transmission spectrum of a broadband light source.^{2,6–9} The other configuration probes the transmission of monochromatic light through nanoholes.^{8,10–15} Because of their small size, nanohole biosensors can be integrated with microfluidic channels to create portable lab-on-a-chip devices.^{6,10,11,15} While EOT nanoholes are compact and sensitive, there are several drawbacks that have prevented either the peak-shift or the light-transmission EOT-based nanohole techniques from being widely used in laboratories or clinical diagnostics. Because of weak optical transmission and diffraction-limited optical resolution, a small array of nanoholes is typically grouped as a single nanosensor, which requires every nanohole of the array to be nearly identical in size and shape.^{1,16,17} This makes them challenging to fabricate and it also is difficult to monitor a large number of sensors simultaneously. Because EOT is very sensitive to shape, size, and local environment of nanoholes, EOT-based techniques require careful design,

precise fabrication, and rigorous spectroscopic characterization of the nanoholes.^{18–21}

In this paper, we report a generic massively parallel method of biosensing using direct nanohole optical imaging. We increased the size of the nanoholes to more than 500 nm so that EOT effects can be neglected. The spacing between the nanoholes is also increased such that individual nanoholes can be resolved and monitored in real-time and in parallel using an ordinary optical microscope. After the capture of biological entities in a nanohole, an enzymatic silver staining step, which is widely used for colorimetric biosensing,^{22–25} is used to partially obstruct the light passing through the opening and darken the hole in the array image. Using UV interference lithography, large-area arrays of nanoholes can be fabricated at a low cost, and more than 10000 nanoholes can be simultaneously monitored and analyzed for in situ sensitive high-speed chemical and biological detection.

EXPERIMENTS AND DISCUSSION

Figure 1 illustrates the transmissive nanohole detection principle. A nanohole array in a gold-coated glass substrate is imaged in transmission mode, and individual nanoholes can

Received: November 7, 2013

Published: February 6, 2014

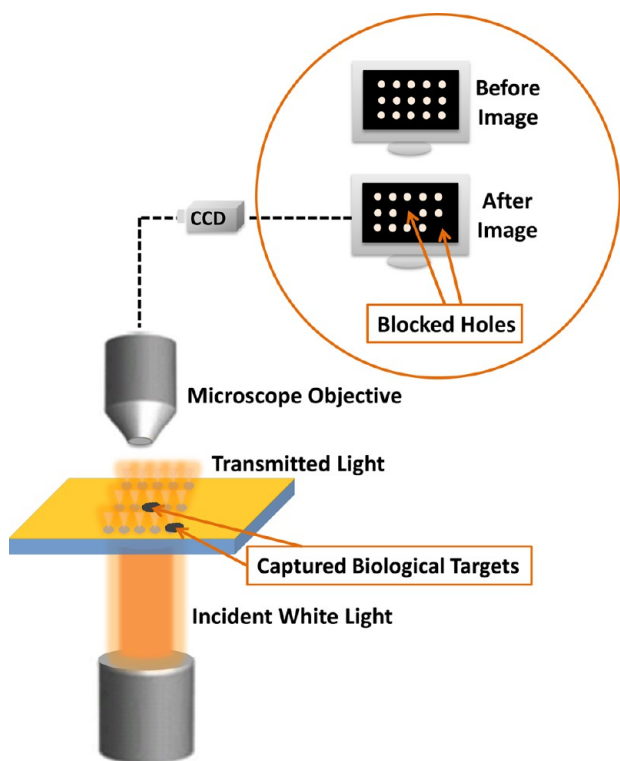


Figure 1. Schematic of the nanohole biosensing approach that combines optical imaging and silver staining. Nanoholes in a gold film are illuminated by white light from the bottom and imaged by a camera through an objective. The “Before Image” and “After Image” stand for images of nanoholes before functionalization and after silver staining, respectively.

easily be resolved as bright spots. A regular array of nanoholes is used in order to facilitate tracking and counting of individual nanoholes. In order to detect a specific biological agent, the glass substrate is functionalized with an appropriate antibody or other capture agent. After the capture of the target analyte in the nanoholes, silver clusters are precipitated around the analyte by enzymatic reactions that attenuate light transmission through the nanoholes, providing a fast and reliable, “digital,” yes/no readout.

Figure 2 shows optical and scanning electron microscope (SEM) images of a nanohole array. The optical image was obtained using white halogen light illumination. The nanoholes appear larger in the optical image than their actual size due to the optical diffraction limit, as shown by comparison with the SEM image. To fabricate a large area nanohole array at low cost, interference lithography was used where a single interference exposure with a 363.8 nm UV laser creates a grating-like pattern. A grid-like pattern is achieved with a second exposure at a 90° rotation. The nanohole size and spacing can be tuned by varying the incident angle of the UV laser and the exposure time. Figure 2c shows an optical image of nearly 10000 nanoholes simultaneously imaged in the field of view of a 50× objective. It should be noted that each nanohole functions as an individual sensor, and thus, we are able to monitor ~10000 individual nanosensors simultaneously.

For a proof of concept, we used hen egg white lysozyme (HEL) as our test analyte. Lysozyme is a canonical model system in immunochemistry, with many well-characterized high-affinity antibodies, obviating any effects of inefficient molecular recognition.^{26,27} In order to apply silver enhance-

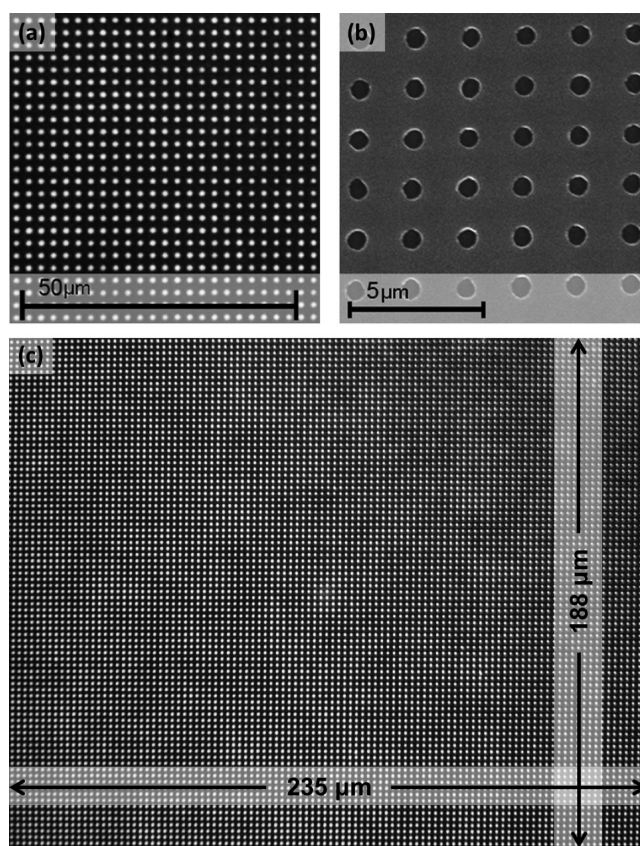


Figure 2. Images of nanohole arrays. (a) Optical transmission and (b) scanning electron microscopy images of nanoholes. (c) Optical transmission image of a total of 8900 nanoholes in the field of view of a 50× objective. The field of $235 \times 188 \mu\text{m}$ is limited by the magnification of the objective and the size of the charge-coupled device (CCD) chip of the camera.

ment, we captured biotinylated-HEL with monoclonal antilysozyme antibodies covalently immobilized in the nanoholes through a silane layer and used streptavidin-horseradish peroxidase (SV-polyHRP) as a reporter to catalyze silver ion reduction and formation of silver clusters around HEL binding sites, using a commercial enzyme metallography detection kit (EnzMet, Nanoprobes Inc.). The details of the experimental procedures are described in the Supporting Information.

The new nanohole biosensing technique works as predicted. Figure 3a shows that several nanoholes are optically blocked in the presence of the analyte and become dimmer or completely

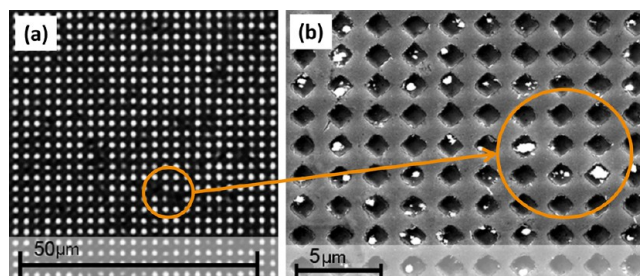


Figure 3. Blocking of nanoholes by enzymatically produced silver precipitates when 100 ng/mL of biotin-HEL was used as a model target. (a) Optical and (b) SEM images of nanoholes after silver staining. The optical transmission of two holes in the circle is blocked, although they are not completely filled with silver precipitates.

dark. A SEM image of the same nanoholes in Figure 3b shows the precipitates in the darkened holes, with a one-to-one correspondence between nanohole transmission blocking and silver precipitates. It should be noted that a nearly total darkening of nanoholes does not require a complete filling with silver precipitates, as indicated by the two nanoholes marked in the circles. Figure S2 in the Supporting Information shows that a small precipitate of silver clusters can also significantly reduce the transmission of a nanohole and can be readily detected.

As expected, the percentage of blocked nanoholes is proportional to the concentration of the analyte, biotin-HEL. Figure 4 shows representative examples of the blocking of

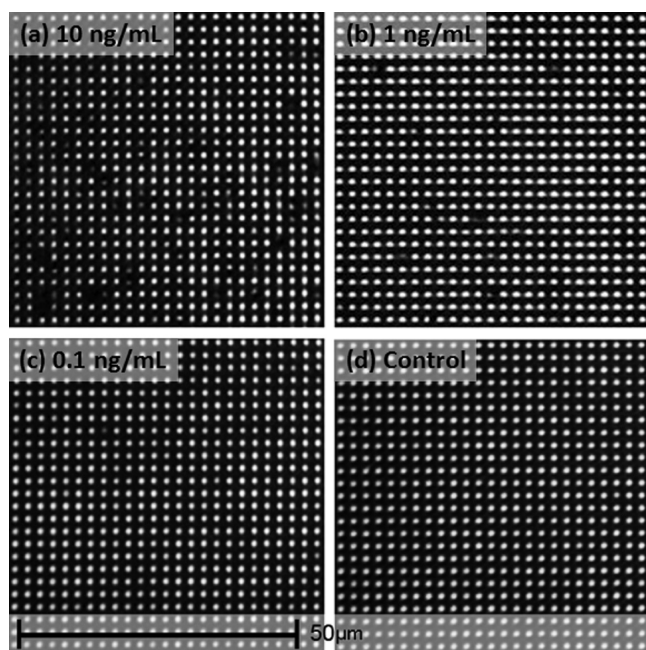


Figure 4. Estimation of the limit of detection (LOD). (a–c) The number of blocked nanoholes decreases at lower concentrations of analyte biotin-HEL. (d) Control experiment with the absence of biotin-HEL shows that no holes are optically blocked.

nanoholes at three different concentrations of biotin-HEL in a $55 \times 55 \mu\text{m}$ area. The number of blocked nanoholes decreases when the concentration decreases. At a concentration of 0.1 ng/mL, only one or very few nanoholes are blocked out of 625 nanoholes. A concentration of biotin-HEL lower than 0.1 ng/mL was not tested, but it is believed that a few blocked nanoholes could be identified in a larger field of view. Because the control experiments consistently show that none of the nanoholes are blocked in the absence of analyte, we estimate that the lower limit of detection in this proof-of-principle experiment is around 0.1 ng/mL. This estimated LOD is not only comparable to EOT-based techniques, but also to other colorimetric methods involving silver enhancement, and even to commercial enzyme-linked immunosorbent assay (ELISA) kits optimized over decades of research.^{4,5,25,28}

This imaging-based nanohole biosensing method is extremely robust and highly resistant to variations and defects in the nanoholes resulting from imperfect fabrication. The SEM pictures in Figures 2b and 3b show that there is a noticeable variation between holes from the same chip, and there is a large difference in nanohole size and shape between two chips fabricated from different batches. The change from smaller

circles in Figure 2b to larger squares in Figure 3b is due to a decreased UV exposure dose.²⁹ However, these fabrication imperfections will not affect the optical imaging readout as individual nanoholes in the same chip can still be clearly identified with very little variation in brightness (Figures S1 and S2 in the Supporting Information), and changes to a single nanohole's optical transmission after silver staining can easily be detected. This technique can also be integrated with microfluidics for real-time in situ monitoring because it requires simple and fast (less than 10 ms per frame) optical imaging.

Silver staining has been widely used for colorimetric detection, where a relatively large sample volume is used. This method can be performed without a microscope, but requires a large volume of staining reagents, and the sensitivity is low.^{30–34} For comparison, we repeated the same functionalization protocol and biotin-HEL assay using $200 \times 200 \mu\text{m}$ holes. Figure 5 shows optical transmission images of

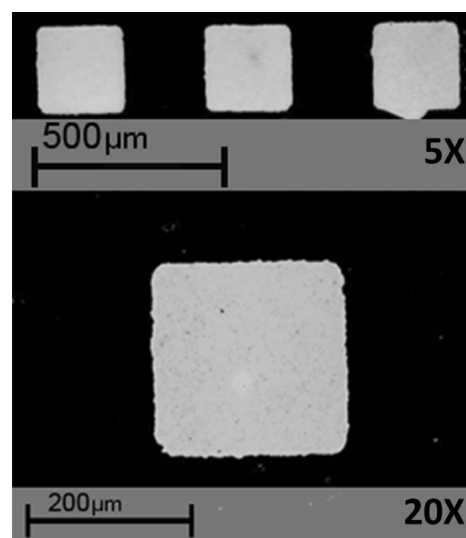


Figure 5. Optical transmission images of $200 \times 200 \mu\text{m}$ silver-stained holes under 5 \times and 20 \times objectives. The 20 \times hole at the bottom is the same as the 5 \times hole on the left.

holes following the same procedure used for nanoholes. The images show that the change in the overall optical transmission is not significant under a low magnification with a 5 \times objective even at a high concentration (10000 ng/mL) of biotin-HEL. Silver clusters, however, become significantly more detectable under a higher magnification with a 20 \times objective. The advantages of nanoholes now become clearer, especially for high sensitivity biosensing. When a small silver cluster precipitates in a large hole, its effect on optical transmission is negligible because of the enormous transmission background, but when a comparable cluster precipitates in a nanohole, it can dramatically reduce the transmission and is much easier to detect. This “digital” ability to track and count individual nanoholes not only simplifies image analysis, but also reduces the rate of false identification.

CONCLUSIONS

We demonstrated a new nanohole-based biosensing technique combining direct nanohole transmission imaging and chemical staining. A low detection limit of 0.1 ng/mL biotin-HEL was achieved in this initial demonstration. The technique is general and can be applied to a wide range of biological agents from

proteins to large pathogens. When combined with microfluidics, the technique should become more compact and efficient and may lead to more practical, real-life clinical diagnostics applications.

■ ASSOCIATED CONTENT

📄 Supporting Information

Experimental details of nanohole fabrication, biofunctionalization protocol, and silver staining; example of image processing. This material is available free of charge via the Internet at <http://pubs.acs.org>.

■ AUTHOR INFORMATION

Corresponding Author

*E-mail: jbao@uh.edu; willson@uh.edu.

Notes

R.W. is an inventor on pending intellectual property filings, which may relate to the content of this paper. The authors declare no competing financial interest.

■ ACKNOWLEDGMENTS

J.B. acknowledges support from the National Science Foundation (DMR-0907336 monitored by Charles Ying, Career Award ECCS-1240510 monitored by Anupama Kaul) and the Robert A. Welch Foundation (E-1728). R.W. acknowledges the support of the NIH WRCE, the Huffington-Woestemeyer Professorship, and the Robert A. Welch Foundation (E-1264). Both J.B. and R.W. acknowledge support of a UH GEAR grant. Support from S. Pei and Center for Advanced Materials are acknowledged.

■ REFERENCES

- (1) Ebbesen, T. W.; Lezec, H. J.; Ghaemi, H. F.; Thio, T.; Wolff, P. A. Extraordinary Optical Transmission through Sub-Wavelength Hole Arrays. *Nature* **1998**, *391*, 667–669.
- (2) Brolo, A. G.; Gordon, R.; Leathem, B.; Kavanagh, K. L. Surface Plasmon Sensor Based on the Enhanced Light Transmission through Arrays of Nanoholes in Gold Films. *Langmuir* **2004**, *20*, 4813–4815.
- (3) Gordon, R.; Sinton, D.; Kavanagh, K. L.; Brolo, A. G. A New Generation of Sensors Based on Extraordinary Optical Transmission. *Acc. Chem. Res.* **2008**, *41*, 1049–1057.
- (4) Escobedo, C. On-Chip Nanohole Array Based Sensing: A Review. *Lab Chip* **2013**, *13*, 2445–2463.
- (5) Valsecchi, C.; Brolo, A. G. Periodic Metallic Nanostructures as Plasmonic Chemical Sensors. *Langmuir* **2013**, *29*, 5638–5649.
- (6) De Leebeek, A.; Kumar, L. K. S.; de Lange, V.; Sinton, D.; Gordon, R.; Brolo, A. G. On-Chip Surface-Based Detection with Nanohole Arrays. *Anal. Chem.* **2007**, *79*, 4094–4100.
- (7) Lesuffleur, A.; Im, H.; Lindquist, N. C.; Oh, S. H. Periodic Nanohole Arrays with Shape-Enhanced Plasmon Resonance as Real-Time Biosensors. *Appl. Phys. Lett.* **2007**, *90*, 243110.
- (8) Henzie, J.; Lee, M. H.; Odom, T. W. Multiscale Patterning of Plasmonic Metamaterials. *Nat. Nanotechnol.* **2007**, *2*, 549–554.
- (9) Kee, J. S.; Lim, S. Y.; Perera, A. P.; Zhang, Y.; Park, M. K. Plasmonic Nanohole Arrays for Monitoring Growth of Bacteria and Antibiotic Susceptibility Test. *Sens. Actuators, B* **2013**, *182*, 576–583.
- (10) Ji, J.; O'Connell, J. G.; Carter, D. J. D.; Larson, D. N. High-Throughput Nanohole Array Based System to Monitor Multiple Binding Events in Real Time. *Anal. Chem.* **2008**, *80*, 2491–2498.
- (11) Lesuffleur, A.; Im, H.; Lindquist, N. C.; Lim, K. S.; Oh, S. H. Laser-Illuminated Nanohole Arrays for Multiplex Plasmonic Microarray Sensing. *Opt. Express* **2008**, *16*, 219–224.
- (12) Yang, J. C.; Ji, J.; Hogle, J. M.; Larson, D. N. Multiplexed Plasmonic Sensing Based on Small-Dimension Nanohole Arrays and Intensity Interrogation. *Biosens. Bioelectron.* **2009**, *24*, 2334–2338.

(13) Lindquist, N. C.; Lesuffleur, A.; Im, H.; Oh, S. H. Sub-Micron Resolution Surface Plasmon Resonance Imaging Enabled by Nanohole Arrays with Surrounding Bragg Mirrors for Enhanced Sensitivity and Isolation. *Lab Chip* **2009**, *9*, 382–387.

(14) Chang, T. Y.; Huang, M.; Yanik, A. A.; Tsai, H. Y.; Shi, P.; Aksu, S.; Yanik, M. F.; Altug, H. Large-Scale Plasmonic Microarrays for Label-Free High-Throughput Screening. *Lab Chip* **2011**, *11*, 3596–3602.

(15) Lee, S. H.; Lindquist, N. C.; Wittenberg, N. J.; Jordan, L. R.; Oh, S. H. Real-Time Full-Spectral Imaging and Affinity Measurements from 50 Microfluidic Channels Using Nanohole Surface Plasmon Resonance. *Lab Chip* **2012**, *12*, 3882–3890.

(16) Ghaemi, H. F.; Thio, T.; Grupp, D. E.; Ebbesen, T. W.; Lezec, H. J. Surface Plasmons Enhance Optical Transmission through Subwavelength Holes. *Phys. Rev. B* **1998**, *58*, 6779–6782.

(17) Weiner, J. The Physics of Light Transmission through Subwavelength Apertures and Aperture Arrays. *Rep. Prog. Phys.* **2009**, *72*, 064401.

(18) Degiron, A.; Lezec, H. J.; Barnes, W. L.; Ebbesen, T. W. Effects of Hole Depth on Enhanced Light Transmission through Subwavelength Hole Arrays. *Appl. Phys. Lett.* **2002**, *81*, 4327–4329.

(19) van der Molen, K. L.; Segerink, F. B.; van Hulst, N. F.; Kuipers, L. Influence of Hole Size on The Extraordinary Transmission through Subwavelength Hole Arrays. *Appl. Phys. Lett.* **2004**, *85*, 4316–4318.

(20) Coe, J. V.; Heer, J. M.; Teeters-Kennedy, S.; Tian, H.; Rodriguez, K. R. Extraordinary Transmission of Metal Films with Arrays of Subwavelength Holes. In *Annu. Rev. Phys. Chem.*; Annual Reviews: Palo Alto, 2008; Vol. 59, pp 179–202.

(21) Li, J. Y.; Hua, Y. L.; Fu, J. X.; Li, Z. Y. Influence of Hole Geometry and Lattice Constant on Extraordinary Optical Transmission through Subwavelength Hole Arrays in Metal Films. *J. Appl. Phys.* **2010**, *107*, 073101.

(22) Holgate, C. S.; Jackson, P.; Cowen, P. N.; Bird, C. C. Immunogold Silver Staining - New Method of Immunostaining with Enhanced Sensitivity. *J. Histochem. Cytochem.* **1983**, *31*, 938–944.

(23) Danscher, G.; Norgaard, J. O. R. Light Microscopic Visualization of Colloidal Gold on Resin-Embedded Tissue. *J. Histochem. Cytochem.* **1983**, *31*, 1394–1398.

(24) Taton, T. A.; Mirkin, C. A.; Letsinger, R. L. Scanometric DNA Array Detection with Nanoparticle Probes. *Science* **2000**, *289*, 1757–1760.

(25) Liu, R.; Zhang, Y.; Zhang, S. Y.; Qiu, W.; Gao, Y. Silver Enhancement of Gold Nanoparticles for Biosensing: From Qualitative to Quantitative. *Appl. Spectrosc. Rev.* **2014**, *49*, 121–138.

(26) Kvasnicka, F. Determination of Egg White Lysozyme by On-Line Coupled Capillary Isotachopheresis with Capillary Zone Electrophoresis. *Electrophoresis* **2003**, *24*, 860–864.

(27) Xiao, Y. H.; Wang, Y. P.; Wu, M.; Ma, X. L.; Yang, X. D. Graphene-Based Lysozyme Binding Aptamer Nanocomposite for Label-Free and Sensitive Lysozyme Sensing. *J. Electroanal. Chem.* **2013**, *702*, 49–55.

(28) Zhang, S.; Garcia-D'Angeli, A.; Brennan, J. P.; Huo, Q. Predicting Detection Limits of Enzyme-Linked Immunosorbent Assay (ELISA) and Bioanalytical Techniques in General. *Analyst* **2014**, *139*, 439–445.

(29) Byun, I.; Kim, J. Cost-Effective Laser Interference Lithography Using a 405 nm Aligned Semiconductor Laser. *J. Micromech. Microeng.* **2010**, *20*, 055024.

(30) Alexandre, I.; Hamels, S.; Dufour, S.; Collet, J.; Zammateo, N.; De Longueville, F.; Gala, J. L.; Remacle, J. Colorimetric Silver Detection of DNA Microarrays. *Anal. Biochem.* **2001**, *295*, 1–8.

(31) Kim, D.; Daniel, W. L.; Mirkin, C. A. Microarray-Based Multiplexed Scanometric Immunoassay for Protein Cancer Markers Using Gold Nanoparticle Probes. *Anal. Chem.* **2009**, *81*, 9183–9187.

(32) Wu, W. Y.; Bian, Z. P.; Wang, W.; Zhu, J. J. PDMS Gold Nanoparticle Composite Film-Based Silver Enhanced Colorimetric Detection of Cardiac Troponin I. *Sens. Actuators, B* **2010**, *147*, 298–303.

(33) Wang, W.; Wu, W. Y.; Zhong, X. Q.; Miao, Q. A.; Zhu, J. J. Aptamer-Based PDMS-Gold Nanoparticle Composite as a Platform for Visual Detection of Biomolecules with Silver Enhancement. *Biosens. Bioelectron.* **2011**, *26*, 3110–3114.

(34) Wen, J.; Shi, X. L.; He, Y. N.; Zhou, J. J.; Li, Y. C. Novel Plastic Biochips for Colorimetric Detection of Biomolecules. *Anal. Bioanal. Chem.* **2012**, *404*, 1935–1944.